

The potentials of mean force of sodium chloride and sodium dimethylphosphate in water: An application of adaptive umbrella sampling

Richard A. Friedman

Department of Biochemistry and Molecular Biophysics, Columbia University, New York, New York 10032

Mihaly Mezei^{a)}

Department of Physiology and Biophysics, Mount Sinai School of Medicine of the City University of New York, New York, New York 10029

(Received 25 May 1994; accepted 19 September 1994)

The potentials of mean force between sodium and chloride ions and between sodium and dimethylphosphate ions in aqueous solution are calculated by the probability ratio method using adaptive umbrella sampling Monte Carlo with a variety of simulation setups. The potential of mean force of sodium chloride is found to have only one minimum in contradiction to earlier molecular dynamics results with the same intermolecular potentials, but different boundary conditions. Our result in the region of contradiction is supported by large system size and free energy perturbation calculations. It is established that the difference is due to the respective boundary condition schemes employed. This result is to be regarded as a consequence of the potential function scheme employed and not necessarily as a statement about actual aqueous sodium chloride. A similar dependence of the existence of the second minimum on boundary conditions is observed for the sodium-dimethylphosphate PMF. © 1995 American Institute of Physics.

I. INTRODUCTION

The effect of solvent molecules on interionic interactions is usually described by adjusting the effective ionic radii of the ions in an analytical thermodynamic theory so as to yield agreement with experimental data.¹ A more realistic approach is the evaluation of the potential of mean force (PMF) $W(r)$ of the interacting ions—the free energy of the interacting ions as a function of distance.²

The magnitude of the electrostatic interaction between two ions is very large—over 100 kcal/mol at 3 Å. In aqueous solution, this interaction, however, is more than overcome by ion–water interactions (since the ions are soluble). Thus the interionic PMF is the result of the balance between O(100 kcal/mol) terms. As a result, the calculated PMF will be influenced uncomfortably by many things (uncomfortable to the theorist, that is).

II. BACKGROUND

PMFs are very difficult to calculate by the probability ratio method using Boltzmann (unbiased) Monte Carlo simulations because of the exponential translation [Eq. (1) *vide infra*] from PMF to probability of occurrence. Each kT drop in the PMF is equivalent to a reduction in the probability of occurrence by a factor of e . To solve this problem, Patey, Valleau, and Torrey introduced the umbrella sampling method, in which the sampling probability is modified by a weighting factor in order to sample regions that are undersampled in Boltzmann Monte Carlo.^{3,4} The efficiency of this method depends on the choice of the weighting function. It is easily shown that the optimum weighting function is

$e^{W(r)/kT}$, where $W(r)$ is the PMF. In other words, in order to calculate the PMF most efficiently, you need to know the PMF to begin with.⁵

To break this vicious cycle, an adaptive technique was introduced independently by Paine and Scheraga⁶ for a molecule in the gas phase and by one of us (M.M.)⁵ for a molecule in solution. In the adaptive umbrella sampling method (AUS), the potential of mean force $W(r)$ is calculated iteratively. First, the simulation settles into a local or global free energy minimum. Then $P(r)$, the probability of two ions being r Angstroms apart is calculated. Finally, an estimated $W(r)$ is obtained from the equation

$$W(r) = -kT \ln P(r) \quad (1)$$

and is then used as a weighting function to sample the undersampled regions. The process is iterated until a targeted region is adequately sampled. Besides the ability of the method to extend the sampled range of $W(r)$, it is inherently self-checking. Recently, Hooft and co-workers developed another variant of the technique and obtained very good results with it.⁷

When the variations in r are the result of the movement of each ion in all possible directions, the geometry of three dimensional space biases the sampling towards large values of r by a factor of $4\pi r^2$ and this bias, when present, must be factored out. In our implementation, however, the relative displacements of the ion were restricted to moves along the straight line passing through the ionic centers. This explains having $P(r) = g(r)$ in Eq. (1) and not $4\pi r^2 g(r)$ as is often seen in similar calculations.

When simulating a liquid system, several choices are made during the simulation setup and several of these affect the calculated energies. First, periodic boundary conditions are imposed to eliminate interfaces from the system. This

^{a)}Author to whom all correspondence should be addressed.

most often takes the form of a cube and its translationally repeated replica, but any geometric object that can be close packed can be used. The cube has often been replaced by a truncated octahedron, or by the Wigner–Seitz cell of the face-centered-cubic (fcc) close packing,⁸ having the advantage that for a given volume, the nearest image–image distance is larger with these shapes than for a cube of the same volume. For PMF calculations, elongated rectangles have also been used. The size of the simulation cell is determined by the number of waters included in the calculations. Also, intermolecular interactions either have to be truncated or some special technique is required for their summation to infinite range, such as the Ewald method.⁹ One truncation scheme, called minimum image (MI),¹⁰ takes into account all interactions between a molecule and the nearest image of all the others. Geometrically, this is equivalent to drawing a cut-off cell of the size of the simulation cell around each molecule. Another truncation scheme, called spherical cutoff (SC)¹⁰ draws a cut-off sphere of radius R_c around each molecule and sets to zero all interactions with molecules farther than R_c . Yet another truncation scheme is the recently introduced isoenergy cut-off method.¹¹ Furthermore, for PMF calculations, the ions can either be considered as separate molecules for the purpose of truncation schemes or as a single molecule.

We would like to propose the view that any setup characteristics that affect the value of the calculated energy of a configuration be considered as part of the potential prescription. There is a qualitative difference between deciding on the acceptance rate or on the time step and on the cut-off radius or the shape of the simulation cell. While most users would hesitate to adjust a potential parameter obtained from a library, most of us consider all set-up decisions as technical detail and make choices accordingly. This is only justified if these choices have a negligible effect on the outcome of the simulation, but the results of this and previous studies show that this is not always the case. Ideally, the latter decisions should have been made at the time of the introduction of the potential.

In this paper, we apply our method to the potentials of mean force of sodium chloride and sodium dimethylphosphate in water. The sodium chloride system was simulated using Jorgensen's TIPS2 potential for H_2O – H_2O interactions¹² and also his potentials for the interactions of Na^+ and Cl^- ions with water and with each other.¹³ This system was chosen to allow comparison with the earlier study with the same potential functions by Berkowitz and co-workers^{14,15} using molecular dynamics. They found a minimum at 5 Å in addition to the contact minimum. Subsequent simulation studies also found a second minimum.^{16–23} Recently, Gao found a second minimum under standard conditions, but found it to vanish under conditions at which water is supercritical.²⁴ A second minimum has also been predicted by integral equation^{25–27} and finite element continuum electrostatics calculations.^{23,28} To the best of our knowledge, there is no experimental evidence for the existence of a second minimum in this system, although Raman spectroscopic evidence has been offered in support of the existence of a second minimum in the PMF of nitrate salts.²⁹

It is interesting to see if the AUS method gives a similar description of the PMF as the dynamics calculations with the same potential functions. As will be seen, there is some disagreement between the results of the two calculations. In the region of disagreement, AUS simulations with a larger box size and/or different cut-off schemes and also free energy perturbation (FEP) calculations were also performed to locate the source of the discrepancies.

Sodium dimethylphosphate is a model system for the study of the ion distribution around DNA. The ion distribution around DNA plays a significant role in the thermodynamics of the binding of drugs and proteins to DNA.^{30–34} Although significant progress has been made in characterizing the ion distribution around DNA at the level of dielectric continuum models, taking into account the effect of discrete water molecules on this distribution is a computationally extensive problem which remains an active area of research. Huston and Rossky studied the effect of bonding contacts on the PMF of Na^+ –DMP[–] in water using free energy perturbation molecular dynamics.³⁵ For motion along the OPO bisector, they found that the second minimum vanished when SC boundary conditions were used, but returned when MI boundary conditions were used. Chen and Rossky derived a PMF similar to the simulation results using integral equation methods.³⁶ In this work, we do calculations on the same system, using a variety of boundary conditions and potential functions.

III. METHODS

The PMF was initially evaluated at 25 °C using one Na^+ – Cl^- ion pair and 215 water molecules in a face-centered cubic box⁸ with an inscribed-sphere radius of 10.4 Å. Interionic distances of between 2.8 and 6.8 Å were sampled. The interionic Lennard-Jones contribution was turned off during the simulation and added in later to save computation.⁴³ The ion pair distance change was obtained by a correlated move of the two ions along the interionic line. Special attention was given to the potential cutoff scheme, as Berkowitz *et al.*¹⁴ warned that the results might change under different boundary conditions and subsequently Huston and Rossky³⁵ found qualitative changes in the PMF when calculations with MI and with SC were compared. The water–water interactions used a 7.5 Å SC.¹⁰ The list of water–water neighbors that might have been within cut-off distance was kept in bitmap form.⁴⁴ SC was not initially used for ion–water interactions because they would lead to an artificial situation in which some of the water molecules interact with the ions and others do not interact with them at all, or, worse yet, interact with only one of the ions. Since for the system under study the ion–water energy at the cutoff can reach 3 kcal/mol the effects can easily be significant. Instead, minimum image boundary conditions were used.¹⁰ However, defining the minimum image in terms of the position of the individual ions can lead to another artificial situation, in which for some of the waters, each of the ions interact with a different periodic replica of it, effectively leading to a situation where a water interacts with one of the ions only. One way to prevent such an artifact is to use a radial cutoff around each ion that is short enough (as was

TABLE I. Characteristics of simulations $\text{Na}^+ - \text{Cl}^-$.

Run	Method	Cell type	Cell size (Å)	Number of H_2O molecules	$\text{H}_2\text{O}-\text{H}_2\text{O}$ cutoff (Å)	Ion- H_2O cutoff (Å)	Second minimum?
<i>A</i>	AUS	fcc	Radius=10.4	215	SPH 7.5	MI (COM)	No
<i>B</i> ^a	AUS	REC	25.5×18.6×18.6	295	SPH 7.5	SPH 7.5	Yes
<i>C</i>	AUS	REC	35.2×22×22	565	SPH 7.5	MI (COM)	No
<i>D</i>	AUS	fcc	Radius=10.4	215	SPH 7.5	SPH 7.5	Yes
<i>E</i>	AUS	REC	25.5×18.6×18.6	295	MI (COM)	MI (COM)	No
<i>F</i>	AUS	fcc	Radius=10.4	215	MI (COM)	MI (COM)	No
<i>G</i>	FEP	fcc	Radius=10.4	215	SPH 7.5	MI (COM)	No
<i>H</i>	AUS	REC	35.2×22×22	565	SPH 7.5	SPH 7.5	Yes
<i>I</i>	AUS	REC	35.2×22×22	565	SPH 9.0	SPH 9.0	Yes
<i>J</i>	AUS	REC	35.2×22×22	565	SPH 10.5	SPH 10.5	Yes
<i>K</i>	AUS	REC	35.2×22×22	565	SPH 7.5	MI (COM)	No
<i>L</i>	AUS	REC	61×22×22	999	SPH 7.5	MI (COM)	No
<i>M</i>	AUS	fcc	Radius=35.2	999	SPH 7.5	MI (COM)	No
<i>N</i>	AUS	REC	35.2×22×22	565	MI (COM)	MI (COM)	Yes
<i>O</i>	AUS	REC	34.2×22×22	549	MI (COM)	MI (COM)	No

^aCorresponds to the conditions of Berkowitz *et al.*

done by Berkowitz *et al.*¹⁴). An alternative way, followed here (for reasons discussed above), defines the minimum image in terms of the center of mass (c.m.) of the ion pair.

Summation to infinity of the periodic replicas (Ewald summation) should be approached with caution. First of all, the artifactual order imposed by the periodic boundary conditions must have some effect on the calculated properties, even for neat liquids where the Ewald sum was reported to perform well.⁴⁵ For the PMF of an ion pair, the problems are exacerbated by the intrinsically large and variable moments of the simulation cell represented by the ion pair. Furthermore, if the ions are of opposite charge, then the simulation cell will have a significant nonvanishing dipole and the electrostatic sum is divergent in principle. Performing Ewald summation for such a system would give a finite value, but it is not clear what that value is, since it is only for unit cells with vanishing dipole that the Ewald sum converges to the electrostatic sum.⁴⁶ This argument rules out Ewald sums (or alternative methods of summing periodic replicas), at least for the PMF between unlike ions.

While in principle a long enough AUS simulation can sample an arbitrarily long interionic distance range, after much effort it was found that it was impossible to sample regions of several Angstroms with the existing biasing techniques. Instead, it was necessary to divide the space into overlapping regions of about 1–2 Å. The following set of sampling parameters was found by trial and error to sample the above regions thoroughly: A *K* parameter of 0.001 [Eq. (20) of Ref. 5] was used to constrain the simulation to an appropriate region. A *C* parameter of 3.0 was used [Eq. (19) of Ref. 5] to extend the simulation to undersampled regions. In addition, the sampling of all previous undersampled regions within the grid were temporarily enhanced by a factor of $e^{1.33}$ as has been described previously.

Simulations in each region were run until the simulation passed smoothly back and forth through the entire region. Regions that initially displayed sudden jumps in the PMF were sampled until the jumps smoothed out. Once a region

seemed adequately traversed, after *n* steps, the simulation was continued for another *n* steps to assure that convergence had taken place. If the PMF had changed substantially, the simulation was continued for another 2*n* steps. This process was continued until convergence was assured. The shape of the PMF was often very different long before convergence was achieved than at convergence. Results for adjacent overlapping regions were matched based on their values in the region of overlap.

The characteristics of the different simulations performed on the NaCl system are summarized in Tables I and II. Run *A* calculates the PMF between 2–7 Å using our boundary conditions of choice: center-of-mass minimum image for ion–water interactions and spherical cutoff for water–water. As will be seen, the results are quite different from those of Berkowitz *et al.* In an effort to isolate the source of the discrepancy between run *A* and the results of Berkowitz *et al.*, further simulations were performed. Run *B* reproduced the calculations of Berkowitz *et al.* over the region of interest with the main exception that AUS Monte Carlo was used rather than molecular dynamics. A cell of identical shape and size was used. For ion–water interactions, a spherical cutoff was used which was computed from the individual ions rather than from the c.m. as in run *A*. Run *C* was an AUS simulation performed in a rectangular box that was 35.15 Å long in the direction of the $\text{Na}^+ - \text{Cl}^-$ distance and 22.0 Å in the other two directions (requiring 565 water molecules). An AUS calculation using a 7.5 Å cutoff on the interactions of each of the ions with water was performed in the fcc cell (run *D*). Calculations in which all interactions were computed according to the minimum image in the rectangular cell (run *E*) and the fcc cell (run *F*) were also performed. To provide an independent check of the AUS method, the slope of the PMF was calculated using the FEP method from the PMF differences over 0.04 Å intervals obtained with 4 million and 3 million Monte Carlo step calculations, respectively, at $r=5.22$ and 6.02 Å in the original simulation box (run *G*). We also performed three calcula-

TABLE II. Region (in Angstroms)/number of steps (M) of windows $\text{Na}^+ - \text{Cl}^-$.

Run	Window 1	Window 2	Window 3	Window 4	Window 5	Window 6	Window 7
<i>A</i>	2.2–3.4/4	3.0–4.6/9	4.4–5.8/12	5.6–7.0/6			
<i>B</i>	5.4–6.3/8	6.2–6.6/5					
<i>C</i>	4.9–6.1/23						
<i>D</i>	6.0–6.9/10						
<i>E</i>	5.4–7.0/15						
<i>F</i>	4.5–5.5/4	5.3–7.0/15					
<i>G</i>	5.22±0.02/4	6.02±0.02/2					
<i>H</i>	6.9–7.5/8	7.5–8.5/8	8.5–9.5/8	9.5–10.5/8	10.5–11.5/8		
<i>I</i>	6.9–7.5/8	7.5–8.5/8	8.5–9.5/8	9.5–10.5/8	10.5–11.5/8		
<i>J</i>	6.9–7.5/8	7.5–8.5/8	8.5–9.5/8	9.5–10.5/8	10.5–11.5/8		
<i>K</i>	6.8–7.4/3	7.4–8.6/5	8.6–9.7/5	9.5–10.6/5			
<i>L</i>	10.4–11.4/8	15.4–16.3/8					
<i>M</i>	11.5–12.5/8	12.5–13.5/8	13.5–14.5/8	14.5–15.5/8			
<i>N</i>	3.5–4.5/8	4.5–5.5/8	5.5–6.5/8	6.5–7.5/8	7.5–8.5/8	8.5–9.5/8	9.5–10.5/8
<i>O</i>	4.5–5.5/8	5.5–6.5/8					

tions in the longer box in the 7–13 Å range using different spherical cut-off radii $R_c = 7.5, 9.0, and 10.5 Å (runs *H*, *I*, and *J*). Minimum image boundary conditions for ion–water and spherical cutoff for water–water interactions in the same box were also employed (run *K*). Also, an even longer (61 × 22 × 22 Å³) rectangular box (run *L*) and a larger (35.2 Å³) fcc box were used (run *M*). Both ion–water and water–water interactions were modeled by minimum image boundary conditions in the 35.15 Å long box (run *N*) and a 1 Å shorter box (run *O*) were also employed. MI/SPH boundary conditions result in each of the ions interacting with different groups of waters than the other one does.⁴⁷ The purpose of run *N* is to test if artifacts result from the use of spherical cut-off boundary conditions for water–water interactions. The purpose of runs *N* and *O*, taken together, is to test if artifacts result from the periodicity of the MI boundary conditions. Runs *A* and *C* used the Metropolis method, while the other runs used the distance-scaled force biased method which had been developed, while this work was in progress, especially for the simulation of ionic solutes.^{48,49} The latter method has been shown to facilitate convergence without sacrificing accuracy.^{48,49}$

The simulation conditions for the $\text{Na}^+ - \text{DMP}^-$ PMF are summarized in Tables III and IV. The DMP^- ion was taken to be in the GC form as was done by Huston and Rossky.

Runs *A'* and *B'* test the sensitivity of the PMF to potential function, using boundary conditions that proved applicable for NaCl. Run *C'* corresponds to the calculations of Huston and Rossky. In this connection, run *C'* uses ion-based (IB) rather than c.m. MI conditions. Runs *E'* and *F'* are the same as *C'* and *D'*, except that the σ 's in the interionic Lennard-Jones potential are determined by a geometric, rather than the usual arithmetic, combination rule.⁵⁰ The arithmetic combination rule makes some physical sense in that the σ 's are proportional to atomic radii, and atomic radii are expected to be additive. We note, in passing, that the Amber,³⁸ OPLS,⁵¹ and GROMOS⁴¹ parametrizations use geometric combination rules.

IV. RESULTS AND DISCUSSION

Figure 1 shows the run *A* results for the PMF excluding interionic Lennard-Jones interactions, the interionic Lennard-Jones contribution, and the total PMF. The raw calculated PMF, which reflects interionic Coulombic plus ion–water and ion–ion interactions has a maximum around 3.36 Å. The decrease of the raw PMF at larger distances reflects the insertion of water molecules between the ions, solvating the ions and pushing them apart. The decrease in the raw PMF at shorter distances reflects the interionic Coulombic

TABLE III. Characteristics of simulations $\text{Na}^+ - \text{DMP}^-$. Amber potential used for DMP^- .^a

Run	Na ⁺ /water potential	Method	Cell type	Combination rule	Cell size (Å)	Number of H ₂ O molecules	H ₂ O–H ₂ O cutoff (Å)	Ion–H ₂ O cutoff (Å)	Second minimum?
<i>A'</i>	Amber ^b /TIPSPC ^c	AUS	fcc	Geometric	Radius=10.4	215	SPH 10.5	MI (COM)	No
<i>B'</i>	OPLS ^d /TIPSPC	AUS	fcc	Geometric	Radius=10.4	215	SPH 10.5	MI (COM)	No
<i>C'</i> ^g	GROMOS ^f /SPC ^f	AUS	fcc	Arithmetic	Radius=10.4	215	MI	MI(IB)	Yes
<i>D'</i>	GROMOS/SPC	AUS	fcc	Arithmetic	Radius=10.4	215	SPH 10.5	MI(IB)	No
<i>E'</i>	GROMOS/SPC	AUS	fcc	Geometric	Radius=10.4	215	MI	MI(IB)	No
<i>F'</i>	GROMOS/SPC	AUS	fcc	Geometric	Radius=10.4	215	SPH 10.5	MI(IB)	Yes

^aCharges (Ref. 33) and Lennard-Jones parameters (Ref. 34).^bReference 39.^cReference 40.^dReference 13.^eReference 41.^fReference 42.^gCorresponds to the conditions of Huston and Rossky.

TABLE IV. Region (in Angstroms)/number of steps (M) of windows, $\text{Na}^+ - \text{DMP}^-$.

Run	Window 1	Window 2	Window 3	Window 4	Window 5
A'	2.36–3.06/4	3.06–3.75/4	3.75–4.45/4	4.45–5.14/4	5.14–5.84/4
B'	2.7–4.3/4	4.1–5.5/4	5.5–6.7/4	6.7–7.9/4	
C'	2.66–3.14/4	2.90–3.78/4	3.62–4.74/4	4.58–5.78/4	5.54–6.74/4
D'	4.58–6.74/4				
E'	2.74–3.78/4	3.62–4.74/4	4.66–5.78/4	5.62–6.74/4	
F'	4.58–6.74/4				

attraction. The decrease in the raw PMF at short distances is balanced out by the Lennard-Jones component which rises rapidly with decreasing distance at short distances. These two countervailing tendencies cause a minimum at 2.88 Å which corresponds to interionic contact. There is no second minimum at about 5 Å as has been predicted by Berkowitz and co-workers^{14,15} and others.^{28,52} We saw such a minimum earlier in our simulation, but it disappeared as the simulation proceeded, implying that it was an artifact caused by insufficient sampling. It is worth emphasizing that our results are consequences of the potential functions used and may not accurately represent the real potential of mean force of the system studied.

The asymptotic behavior of the PMF at large distances is expected to be given by Coulomb's law with a dielectric constant equal to that of bulk water. However, between 3.5 and 7 Å, at most one and a half water molecules can fit between the ions. Hence, the ions are not fully solvated, so that we do not expect the system to behave the same as point ions surrounded by a dielectric continuum. Rather, the PMF

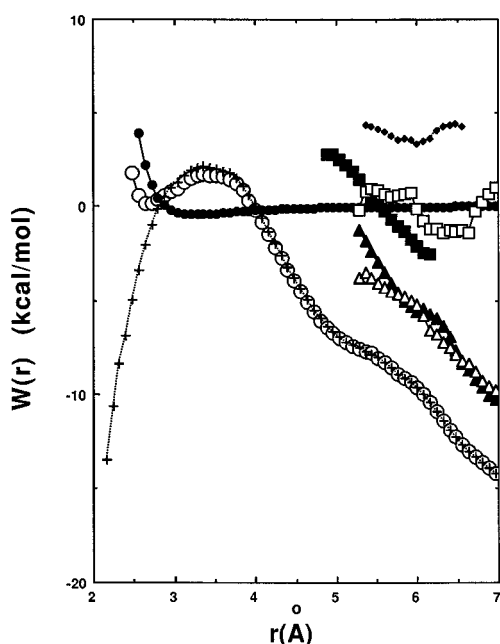


FIG. 1. PMF of $\text{Na}^+ - \text{Cl}^-$ in H_2O at 25 °C. (run A) total PMF \circ ; ion–water Coulombic and ion–water Lennard-Jones contributions, +; ion–ion Lennard-Jones contribution \bullet . All of the other runs are total PMFs. (run B) \blacklozenge ; (run C) \blacksquare ; (run D) \square ; (run E) \blacktriangle ; (run F) \triangle . The absolute energies of the runs are offset for clarity.

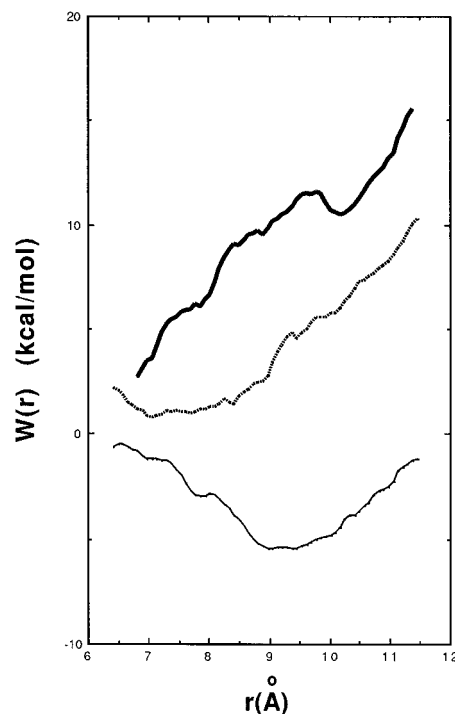


FIG. 2. Total PMF of $\text{Na}^+ - \text{Cl}^-$ in H_2O at 25 °C. The effect of the spherical cutoff on the location of second minimum. (run H)—; (run I) ···; (run J) —.

decreases significantly because the ions become more solvated with increasing distance. The slope of the PMF in this region is steep, because the solvation free energy of the sodium and chloride ions is large, reflecting the fact that sodium chloride is very soluble in water.

Runs B–O repeat run A over the contested region, and beyond, according to differences in box size, shape, and boundary conditions (Figs. 1–4). Whether or not a run gives a second minimum is summarized in Table I. Among runs B–M, only those runs that employ spherical ion–ion cutoffs exhibit a second minimum and the position of the second minimum is correlated with the cut-off length. This result implies that for this system and potential function set, the second minimum can appear as an artifact of the use of a spherical cutoff for ion–water interactions. The FEP results (run G) show that the slope of the PMF was 4.2 and 3.0 kcal/mol/Å at 5.02 and 6.02 Å, respectively. Thus the FEP calculations also do not exhibit a second minimum. Runs H, I, and J test the effect of varying the spherical cutoff on a larger box. The solvent-separated minimum appears to move out in correlation with the increase in the cut-off radius. We consider this to be strong evidence in particular that in this system, the solvent-separated minimum is an artifact of the SC and in general that SC is likely to introduce significant artifacts into the results. Calculations in yet larger boxes produce similar results (runs L and M) and the PMF finally levels off in the 62 Å long box after 15 Å. Assuming bulk dielectric behavior at 15 Å, the contribution to the PMF from solvent screened ion–ion interactions is about one quarter of a kilocalorie, which is well within the error of our simulations. Hence the observed curves approximate the long-range

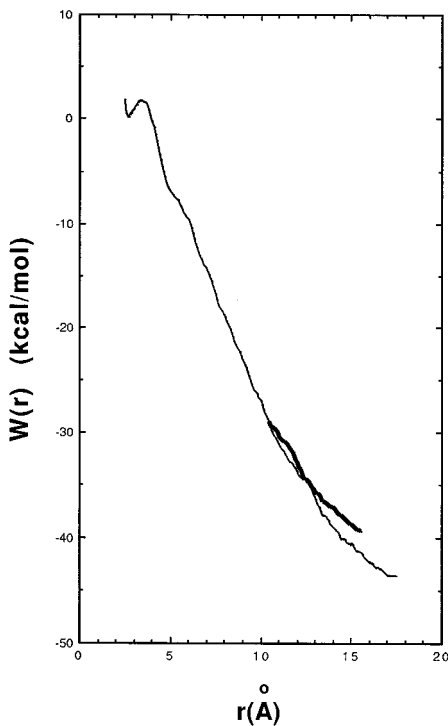


FIG. 3. Total PMF of $\text{Na}^+–\text{Cl}^-$ in H_2O at 25°C over a wider scale. MI/SPH 7.5 boundary conditions (runs A , K , L)—; (run M)—.

bulk dielectric limit. However, that the PMF is repulsive at such long distances is probably an artifact of the potential function used.²⁵ Perhaps the disagreement with an integral equation treatment of this system is due to differences in the

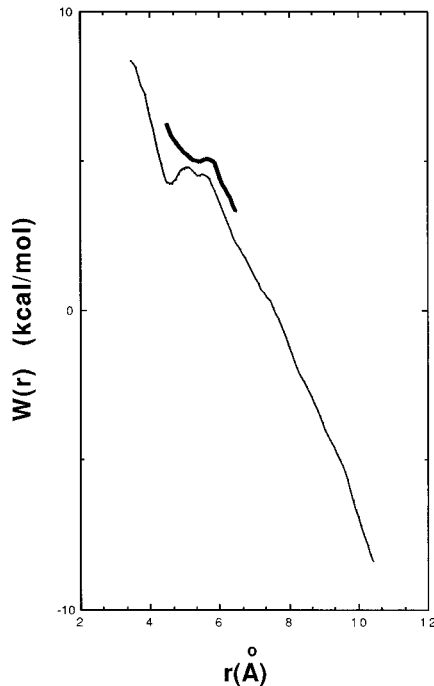


FIG. 4. Total PMF of $\text{Na}^+–\text{Cl}^-$ in H_2O at 25°C . (run N)—; (run O)—.

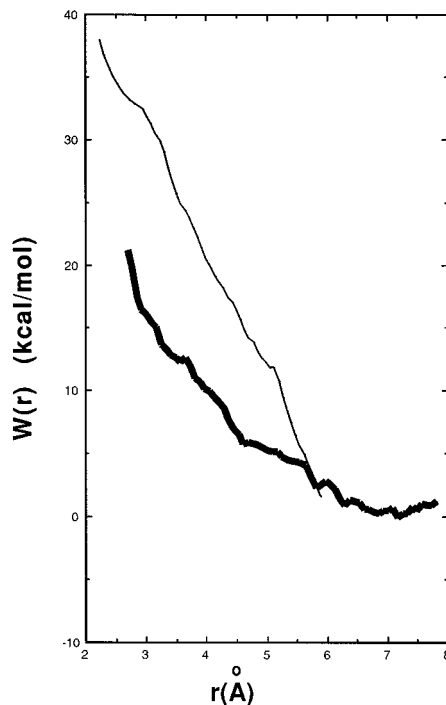


FIG. 5. Total PMF of $\text{Na}^+–\text{DMP}^-$ in H_2O at 25°C . (run A')—; (run B')—.

potential functions used in the two studies. Run N (MI/MI) exhibits a second minimum. This run, taken alone, might be taken to imply that the lack of the second minimum in the previous runs employing mixed MI/SPH boundary conditions were an artifact of the effect discussed by Huston and Rossky (see above).³⁵ However, run O which is identical to run N , except that the box is 1 Å shorter, does not exhibit a second minimum, at least at the same location as in run O . This result indicates that MI/MI boundary conditions are also subject to artifacts, perhaps arising from each ion interacting with water polarized by the images of the other ion.

The $\text{Na}^+–\text{DMP}^-$ PMF in TIP4P water gave similar results to the $\text{Na}^+–\text{Cl}^-$ calculations in that the PMF shows a large drop from the contact distance, but that no second minimum is exhibited (run A' in Fig. 5). Changing the Na^+ parameter produced a quantitative change in the PMF, including a reproduction of Coulombic behavior, but no well-defined second minimum (Fig. 4). Also changing the water potential gave a significantly smaller drop (runs $C'–F'$ in Fig. 6). Like Huston and Rossky, we obtained a second minimum using minimum image boundary conditions with the arithmetic combination rule. The final comparison concerned the use of SC and MI on the solvent–solvent interactions and the choice of the Lennard-Jones combination rule. The simulations show that both have a significant effect on the results. Indeed, the geometric combination rule with spherical cut-off boundary conditions also yields a second minimum. As we have demonstrated in the case of the $\text{Na}^+–\text{Cl}^-$ PMF, the ability to reach long range behavior within simulation error over a physically reasonable distance depends on potential function. We have not run these simulations in longer boxes until limiting behavior is demonstrated.

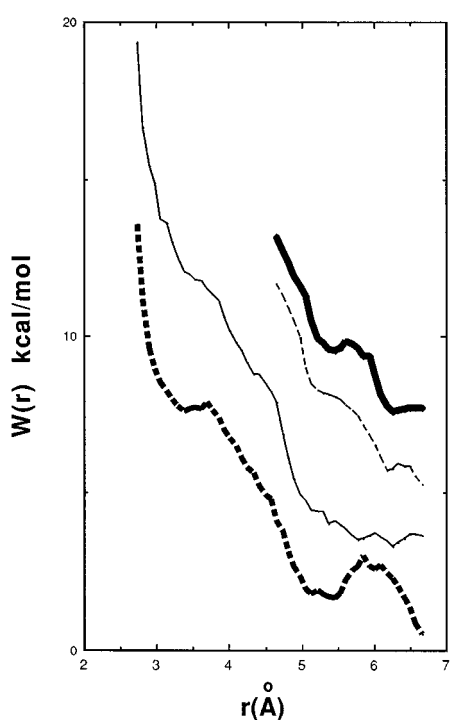


FIG. 6. Total PMF of $\text{Na}^+ - \text{DMP}^-$ in H_2O at 25°C . (run C')—; (run D')---; (run E')—.; (run F')—.

V. CONCLUSIONS

The calculations presented here provide additional strong evidence of the very strong sensitivity in interionic PMFs to the model chosen. The simulation setup advocated by us appears to give results independent of the simulation box size and shape, a promising result. Careful reparametrization of the potential parameters is required, keeping the set-up variables the same all the way.

For the determination of the best set-up conditions, further research is needed. This would involve a comparison of results using various setups with results from a system large enough to be considered "infinite." The best setup would reproduce the "infinite" system size result with the smallest system size. Based on the arguments presented in this paper, we expect that the setup advocated here will be among the best according to this criterion.

Whether or not a solvent separated second minimum is present is the result of a delicate balance between solute–solute and solvent–solvent interactions and the simulation protocol used. For example a previous simulation of the $\text{Na}^+ - \text{Cl}^-$ PMF showed a second minimum, but in our hands, a nonphysical interionic repulsion at long distances was observed.

ACKNOWLEDGMENTS

This work was supported by a CUNY-PSC grant and an NIH Shannon award (R55-GM43500) to M.M., an NIH/RCMI grant (SRC5G12RR0307) to Hunter College. R.A.F.'s involvement was supported in part by NIH grant (GM-41371). Computing resources were provided in part by the NSF supercomputer center at Pittsburgh and by the University

Computing Center of the City University of New York. We thank Dr. Andrew Pohorille for a helpful discussion and Dr. Peter Rossky for helpful correspondence. This paper is dedicated to the memory of our friend and colleague Dr. David Belford.

- ¹J. O. Bockris and A. K. N. Reddy, *Modern Electrochemistry* (Plenum, New York, 1979), p. 219.
- ²D. A. McQuarrie, *Statistical Mechanics* (Harper & Row, New York, 1976), p. 264.
- ³G. N. Patey and J. P. Valleau, *J. Chem. Phys.* **63**, 2334 (1975).
- ⁴G. Torrie and J. P. Valleau, *J. Comput. Phys.* **23**, 187 (1977).
- ⁵M. Mezei, *J. Comput. Phys.* **68**, 237 (1987).
- ⁶G. H. Paine and H. A. Scheraga, *Biopolymers* **24**, 1391 (1985).
- ⁷R. W. W. Hooft, B. P. Van Eijck, and J. Kroon, *J. Chem. Phys.* **97**, 6690 (1992).
- ⁸J. C. Owicki and H. A. Scheraga, *J. Am. Chem. Soc.* **99**, 8382 (1977).
- ⁹M. P. Allen and D. J. Tildesley, *Computer Simulation of Liquids* (Oxford, Oxford, 1989), p. 156.
- ¹⁰M. P. Allen and D. J. Tildesley, *Computer Simulation of Liquids* (Oxford, Oxford, 1989), p. 27.
- ¹¹M. Mezei, *Int. J. Quantum Chem.* **52**, 147 (1994).
- ¹²W. L. Jorgensen, *J. Chem. Phys.* **77**, 4156 (1982).
- ¹³J. Chandrasekhar, D. C. Spellmeyer, and W. L. Jorgensen, *J. Am. Chem. Soc.* **106**, 903 (1984).
- ¹⁴M. Berkowitz, O. Karim, J. McCammon, and P. J. Rossky, *Chem. Phys. Lett.* **105**, 577 (1984).
- ¹⁵A. C. Belch, M. Berkowitz, and J. A. McCammon, *J. Am. Chem. Soc.* **108**, 1755 (1986).
- ¹⁶J. Van Eerden, W. J. Biels, S. Harkema, and D. Feil, *Chem. Phys. Lett.* **164**, 370 (1989).
- ¹⁷L. X. Dang, J. E. Rice, and P. A. Kollman, *J. Chem. Phys.* **93**, 7528 (1990).
- ¹⁸E. Guardia, R. Rey, and J. A. Padro, *Chem. Phys.* **155**, 187 (1991).
- ¹⁹S.-B. Zhu and G. W. Robinson, *J. Chem. Phys.* **97**, 4336 (1992).
- ²⁰D. E. Smith and L. X. Dang, *J. Chem. Phys.* **100**, 3757 (1993).
- ²¹G. Hummer, D. M. Soumpasis, and M. Neumann, *Mol. Phys.* **77**, 769 (1992).
- ²²G. Hummer, D. M. Soumpasis, and M. Neumann, *Mol. Phys.* **81**, 1155 (1994).
- ²³L. R. Pratt, G. Hummer, and A. E. Garcia, *Biophys. Chem.* **51**, 147 (1994).
- ²⁴J. Gao, *J. Phys. Chem.* **98**, 6049 (1994).
- ²⁵B. M. Pettitt and P. J. Rossky, *J. Chem. Phys.* **84**, 5836 (1986).
- ²⁶J. S. Perkyns and B. M. Pettitt, *Chem. Phys. Lett.* **190**, 626 (1992).
- ²⁷J. Perkyns and B. M. Pettitt, *J. Chem. Phys.* **97**, 7656 (1992).
- ²⁸A. Rashin, *J. Phys. Chem.* **93**, 4644 (1989).
- ²⁹P. D. Spohn and T. B. Brill, *J. Phys. Chem.* **93**, 6224 (1989).
- ³⁰G. S. Manning, *Q. Rev. Biophys.* **11**, 179 (1978).
- ³¹M. T. Record, C. F. Anderson, and T. M. Lohman, *Q. Rev. Biophys.* **11**, 103 (1978).
- ³²R. A. Friedman and G. S. Manning, *Biopolymers* **23**, 2671 (1984).
- ³³V. K. Misra, J. L. Hecht, K. A. Sharp, R. A. Friedman, and B. Honig, *J. Mol. Biol.* **238**, 264 (1994).
- ³⁴V. K. Misra, K. A. Sharp, R. A. Friedman, and B. Honig, *J. Mol. Biol.* **238**, 245 (1994).
- ³⁵S. E. Huston and P. J. Rossky, *J. Phys. Chem.* **93**, 7888 (1989).
- ³⁶S.-w. W. Chen and P. J. Rossky, *J. Phys. Chem.* **97**, 6078 (1993).
- ³⁷G. Alagona, C. Ghio, and P. A. Kollman, *J. Am. Chem. Soc.* **107**, 229 (1985).
- ³⁸S. J. Wiener, P. A. Kollman, D. A. Case, U. C. Singh, C. Ghio, G. Alagona, S. Profeta, and P. Weiner, *J. Am. Chem. Soc.* **106**, 765 (1984).
- ³⁹T. Lybrand and P. Kollman, *J. Chem. Phys.* **83**, 2923 (1985).
- ⁴⁰W. L. Jorgensen, J. Chandrasekhar, J. D. Madura, R. W. Impey, and M. L. Klein, *J. Chem. Phys.* **79**, 926 (1983).
- ⁴¹W. F. Van Gunsteren and H. J. C. Berendsen, *GROMOS86 Groningen Molecular Simulation Systems* (Groningen University, Groningen, 1986).
- ⁴²H. J. C. Berendsen, J. P. M. Postma, W. F. Van Gunsteren, and J. Hermans, *Intermolecular Forces* (Reidel, Amsterdam, 1981).
- ⁴³M. Mezei and D. L. Beveridge, *Ann. Acad. Sci. N.Y.* **482**, 1 (1986).
- ⁴⁴M. Mezei, *Mol. Simul.* **1**, 169 (1988).
- ⁴⁵D. J. Adams, *Chem. Phys. Lett.* **62**, 329 (1979).

⁴⁶ E. S. Campbell, *J. Phys. Chem. Solids* **24**, 197 (1963).

⁴⁷ P. J. Rossky (personal communication, 1994).

⁴⁸ M. Mezei, *Mol. Simul.* **5**, 405 (1991).

⁴⁹ M. Rao, C. S. Pangali, and B. J. Berne, *Mol. Phys.* **37**, 1779 (1979).

⁵⁰ J. P. Hansen and I. R. MacDonald, *Theory of Simple Liquids* (Academic, London, 1990), p. 179.

⁵¹ W. L. Jorgensen and J. Tirado-Rives, *J. Am. Chem. Soc.* **110**, 1657 (1988).

⁵² F. Hirata, P. J. Rossky, and B. M. Pettitt, *J. Chem. Phys.* **78**, 4133 (1983).